JOURNAL OF APPLIED ELECTROCHEMISTRY 24 (1994) 554–558

# Preparation of electrolytic ceramic films on stainless steel conversion coatings

L. ARIES

*Equipe de Métallurgie Physique, Laboratoire des Matériaux (URA CNRS 445), Ecole Nationale Supérieure de Chimie (INPT), 118 route de Narbonne, 31077 Toulouse Cedex, France*

Received 19 April 1993; revised 22 November 1993

An electrolytic method for the synthesis of an alumina barrier on stainless steel with strong interfacial bonding is described for a Fe–17%Cr alloy. The deposit was laid down electrochemically after a specific conversion treatment by chemical oxidation of the substrate in acid solution. The conversion coating was very porous and had excellent adhesion at the substrate interface. Alumina was obtained by thermal dehydration of aluminium hydroxide deposited from an aqueous solution of an aluminium salt, according to a two-step mechanism: generation of hydroxyl ions at the cathodic substrate by reduction of $H_2O$ or dissolved oxygen and a precipitation reaction forming aluminium hydroxide. Thermal treatment induced interfacial reactions between aluminium oxide and conversion coating compounds which led to spinel formation beneath the superficial alumina layer. The coating presented chemical composition gradients suitable for strong adhesion. Thermal oxidation resistance was studied in air at 1000° C.

## 1. Introduction

The use of ceramic coatings to protect and insulate metals from high-temperature corrosive environments is of great interest. They improve the performance and efficiency of heat engines, allowing the use of higher engine temperatures and decreasing the oxidation rate. Generally, ceramic coatings are obtained by techniques like plasma spraying, chemical vapour deposition, sputtering [1, 2] and sol–gel processes [3, 4] or by multiple applications of an appropriate solution and firing [5]. Ceramic films or powder can also be obtained by electrochemical means [6–13]. The equipment is of low cost and controlling the thickness, the morphology and the properties of the coating on complex shapes is very easy, by varying electrochemical parameters and bath composition. Barrier coatings are made up of materials which must satisfy several criteria: high thermal stability, low thermal conductivity and, particularly, thermal expansion equal to that of the substrate. Thus, one problem is coat adhesion, which restricts the choice of the ceramic. To strengthen the interface between ceramic and substrate, an original specific pretreatment of the metal surface is proposed so as to form a functional conversion coating characterized by strong interfacial adhesion with the substrate and by properties enabling interfacial reaction at high temperatures with the ceramic coating. The reaction products must act as a bond between the substrate and the ceramic coating. Moreover, the morphology of the surface is important [14]. The conversion coating must be very porous to contribute to the 'anchoring' of the ceramic layer and to facilitate the interfacial reactions. It must be also a conducting material so that the ceramic coating can be formed by electrochemical means.

In this paper the electrochemical synthesis of an alumina barrier coating on stainless steel through a conversion coating is presented.

## 2. Experimental details

The deposits were obtained on a Fe–17%Cr ferritic stainless steel (French standard Z8 C17); its composition is given in Table 1. Substrates were prepared in the form of 0.6 mm × 20 mm × 50 mm specimens. The original surface state of the steel sheets was preserved. The samples were cleaned with ethanol, washed with distilled water and then dried in air at room temperature. Details of the solution, chemical compositions, bath temperature and electrochemical parameters, are described for each treatment.

A Tacussel potentiostat PRT 20-02 fitted with a pilot scanner was used to obtain polarization curves ($10\,mV\,min^{-1}$). Electrode potentials were measured with a high input impedance voltmeter ($10^{12}\,\Omega$), Tacussel MVN 82. A saturated calomel electrode was used as reference.

A high temperature oxidation experiment was carried out in air. The gain in weight of the specimens was determined with a Setaram B24 Netzsch thermobalance. The distribution profiles of elements in the coatings was obtained with a SIMS method using an IMS 300 Cameca analyser. The diameter of the circular zone analysed was about 25 $\mu$m; metalloid profiles were obtained in inert atmosphere by bombardment with an argon gun. Metal signals were maximized by maintaining the oxygen level in the analysis chamber at a very low value.



0021-891X 

*Table 1. Chemical composition of the stainless steel used*

| Element | Si | Mn | Cr | Mo | Ni | Al | Cu | Nb | Ti | Fe |
|---|---|---|---|---|---|---|---|---|---|---|
| wt % | 0.49 | 0.19 | 15.99 | 0.13 | 0.24 | 0.12 | 0.34 | 0.17 | 0.02 | Bal. |

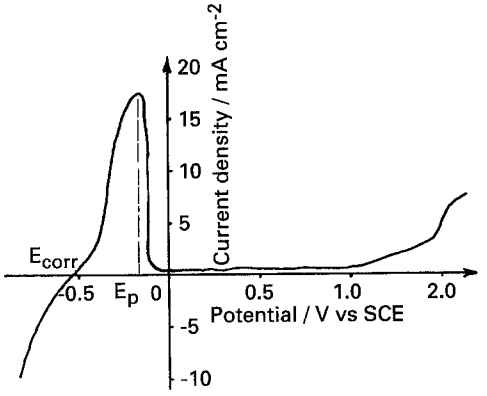


Fig. 1. Polarization curve for Fe–17%Cr alloy in the treatment bath.

## 3. Chemical conversion coating

### 3.1. *Preparation*

Stainless steel conversion coatings can be obtained either by electrolytic or chemical treatment in an acid bath containing suitable additives and, particularly, substances containing chalcogenides such as sulphur (sulphides, thiosulphates) [15–19]. Corrosion inhibitors like acetylenic alcohols are also required to facilitate the control of film growth in order to obtain coats with specific properties. With the electrolytic route, the treatment is carried out by controlling the electrode potential. The anodic oxidation of the surface is carried out at a potential corresponding to the activity domain: between the corrosion potential $E_{corr}$ and the primary passivity potential $E_p$ (Fig. 1) of the alloy dipped in the treatment bath. In the chemical route the conversion coating is obtained by dipping the stainless steel into the bath. The electrode potential of the steel must be controlled because one of the main conditions of the treatment is the fitting of its value to that of the corrosion potential in the active state. This potential condition is often naturally fulfilled for the treatment baths used. If not, adjustment of the potential to the required value can be accomplished by the cathodic activation of the surface in the treatment bath for a few minutes.

In the present study, the coatings were obtained by chemical treatment of Fe–17%Cr stainless steel in a sulphuric acid solution (pH 0) with 130 p.p.m. $S^{2-}$ and propargyl alcohol ($6 \times 10^{-2}$ M) as inhibitor.

The polarization curve on the steel in the treatment bath is shown in Fig. 1. The corrosion potential was about −500 mV. Cathode activation of the surface was not necessary to prepare the chemical conversion coating. The variation in electrode potential of the sample during the treatment indicates two phases (Fig. 2). During the first phase the electrode potential decreases quickly from positive values to −515 mV: this phase corresponds mainly to the dissolution of the passive film naturally formed in air; formation of the conversion coat starts on the free surface [19]. In the second phase, the electrode potential increases very slowly; this corresponds to the growth of the conversion coating.

### 3.2. *Chemical composition*

The plot of the SIMS profiles versus bombardment time shows a concentration gradient of metallic elements in the coating (Fig. 3). The coatings are characterized by a continuous variation of the chemical composition from the metallic substrate to the superficial zone. Moreover, Fe and Cr present identical profiles, which suggests that they are part of the same chemical compound. In previous work, it was shown, using infrared spectrometry and X-ray diffraction, that the main component of this kind of coating is a substituted magnetite $(Fe^{2+}Fe^{3+}_{2-x}Cr^{3+}_{x})O^{2-}_{4}$, probably oxidized to varying degrees according to its depth in the coat [20–22]. The superficial oxidation of the coating could lead to $\gamma$ $(Fe^{3+}_{1-y}Cr^{3+}_{y})_2O^{2-}_{3}$. These phases are in the amorphous state.

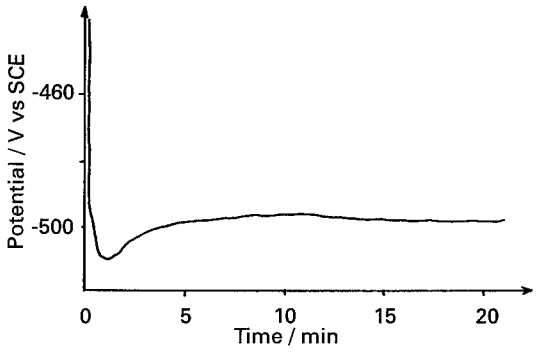


Fig. 2. Electrode potential against treatment time.

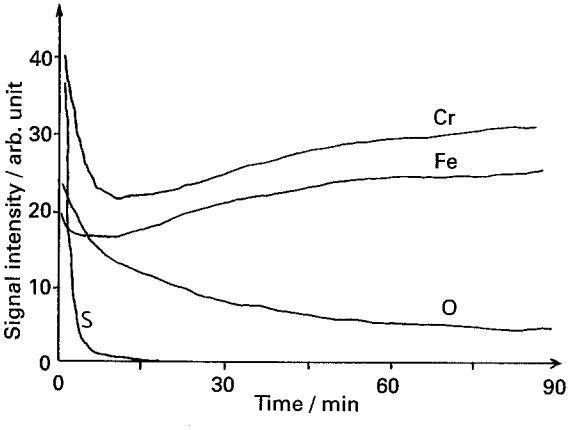


Fig. 3. Distribution profiles of the elements in the initial conversion coating against bombardment time.

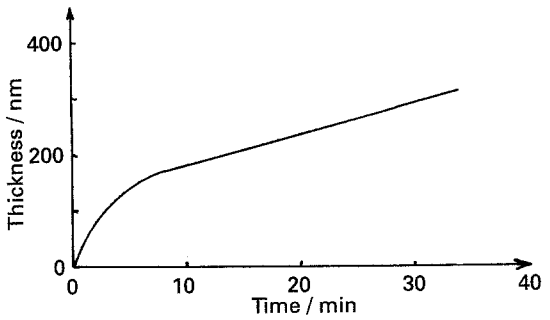


Fig. 4. Coating thickness against treatment time.

### 3.3. *Thickness and morphology*

Conversion coating thickness was evaluated from the sputtering time by ionic bombardment (SIMS), assuming that the sputtering rate did not differ with the analysed depth. The thickness increased with the treatment time as indicated in Fig. 4. The rate of growth of the conversion coating decreased during the treatment and became constant. After 20 min, the thickness was about 200 nm. Visually, the conversion coating appeared homogeneous. Examination by scanning electron microscopy showed that the layer had a uniform appearance; the surface was very rough and had pores and cavities with a range of dimensions. The same type of irregularity was noted on different scales of observation. This suggests that the conversion coatings have a fractal character. The correlation between the electrochemical behaviour of the conversion coatings and their thermal oxidation was studied previously [22, 23].

## 4. Electrodeposition of aluminium hydroxide

### 4.1. *Preparation*

Oxides and hydroxides are commonly deposited by electrooxidation reactions induced on the anode [24]. They can also be obtained through cathodic reactions with a process involving both electrochemical and chemical reactions [10–12].

The present work deals with the deposition of aluminium hydroxide from a saturated aqueous solution of aluminium sulphate. The hydroxide may be formed in two successive steps:

(i) Generation of $OH^-$:

$$2H_2O + 2e^- \longrightarrow H_2 + 2OH^-$$

If the cathode is a porous electrode, like the stainless steel conversion coating, this reaction may occur at the bottom of the pores with a resulting local rise in pH.

Hydroxyl ions $OH^-$ can also be generated by reduction of dissolved oxygen according to

$$O_2 + 2H_2O + 4e^- \longrightarrow 4OH^-$$

(ii) Precipitation of aluminium hydroxide by interaction of $Al^{3+}$ with $OH^-$ ions:

$$Al^{3+} + 3OH^- \longrightarrow Al(OH)_3$$

The deposit can be fired in order to induce the dehydration of the hydroxide and the formation of alumina:

$$2Al(OH)_3 \longrightarrow Al_2O_3 + 3H_2O$$

The substrate was always Fe–17%Cr stainless steel with a chemical conversion coating prepared according to the chemical method mentioned earlier. For aluminium hydroxide deposition, a platinum electrode was used as anode. Deposits were obtained at electrode potentials ranging from 3 to 5 V and durations of 15 to 60 min. Coating thickness was controlled by varying the duration of the process. Experiments were performed without stirring.

The dependence of current density on deposition time is shown in Fig. 5 for a cell voltage of 3 V, the current density decreased with deposition time and was practically stable after 30 min at about 12 mA $cm^{-2}$. This behaviour was related to the mechanism of the deposit formation.

In the first stage of the deposition process, the conversion coating substrate being conductive, electrochemical reaction (i) occurs over its entire surface and especially at the bottom of the pores, near the metal, where the electrical resistance of the coating is lowest. The deposition progresses until the pores are filled with precipitate according to reaction (ii). During this stage, the electrical resistance of the conversion coating, modified with aluminium hydroxide increases. This variation of the coating induces a decrease in the current density at constant voltage.

In the second stage the deposit continues to form, the thickness of the coating increases, while hydrogen

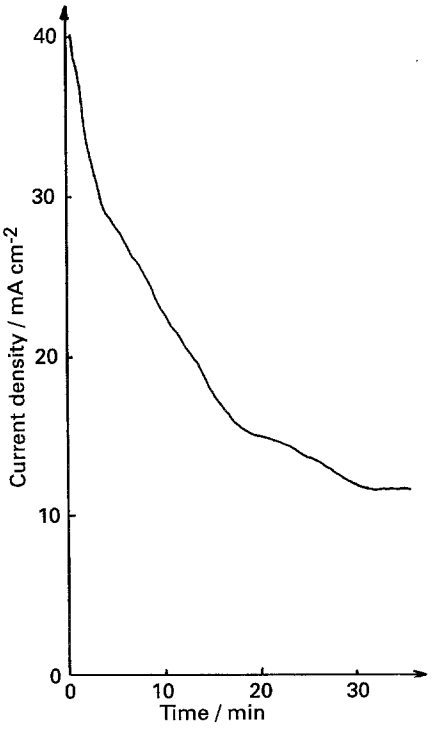


Fig. 5. Current density against deposition time.

release can still be seen at the surface. During this stage, the current density decreases, due to coating thickening. However, its value remains high during the whole of coating production (60 min), showing that the coat is still porous, probably owing to hydrogen release which takes place at sites of lower electrical resistance. Thus, the deposit is made of two layers: the deep zone consists of the conversion coating modified by aluminium hydroxide and the superficial zone is constituted by the aluminium hydroxide deposit alone.

The increase in electric resistance caused by the formation of the deposit leads to a rise in solution temperature, which may affect the electrode processes. Thus, the temperature must be controlled.

### 4.2. *Surface analysis*

SIMS profiles of a thin deposit (15 min, 3 V) shows that the aluminium ratio is very high at the coating surface and that this element has diffused into the conversion coating up to the stainless steel substrate (Fig. 6). Profiles of iron and chromium from the initial conversion coating are not strongly modified by the cathodic post-treatment. The distribution of these three elements is a favourable factor for strong ceramic adhesion. Thick deposits were composed of two layers. The deep layer is described above (conversion coating modified by aluminium hydroxide): its thickness was that of the initial conversion coating. The superficial layer constituted only of aluminium hydroxide: its thickness increased with deposition time.

The coating composition supports the mechanism proposed.

### 4.3. *Resistance to thermal oxidation*

Figure 7 shows the weight change with time curves for the uncoated and coated Fe–17%Cr alloy specimens oxidized in air at 1000° C. The resistance to oxidation of the coated alloy is high compared to that of the uncoated alloy. The poor oxidation resistance at

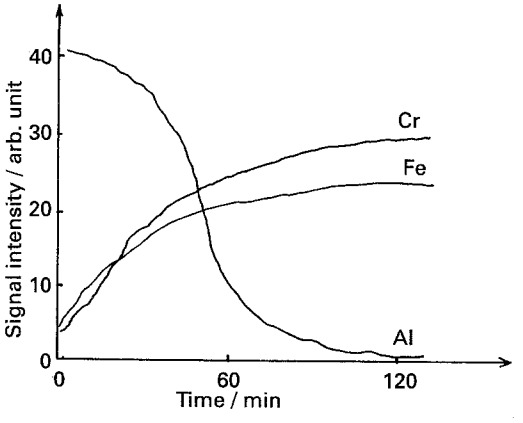


Fig. 6. Distribution profiles of the elements in the modified conversion coating against bombardment time.

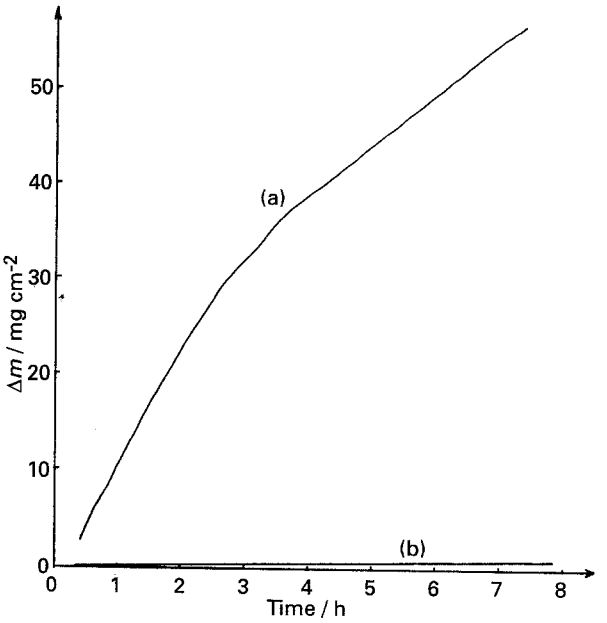


Fig. 7. Gain in weight of coating against thermal treatment time in air at 1000° C. (a) uncoated alloy, (b) ceramic coated alloy.

1000° C of the Fe–17%Cr alloy is due to its too low chromium content, which allows the formation of a $Cr_2O_3$ layer inclined to scaling. Moreover, above 1000° C the $Cr_2O_3$ may volatilize. The coated specimen exhibits a low oxidation rate owing to the formation of an $\alpha Al_2O_3$ oxide barrier at the surface. This outer layer of the coating is very adherent because of reactions between the alumina deposit and the iron–chromium oxides of the stainless steel conversion coating. These reactions induce the formation of a spinel structure $(Fe^{2+}Al^{3+}_{2-y}Cr^{3+}_{y})O^{2-}_{4}$ in the inner layer with a concentration gradient which varies according to the depth [25].

To verify the high thermal shock resistance of the coating, the specimen was alternately heated in an oven at 1000° C and withdrawn from it every three minutes; any damage of the surface was noted after 200 cycles.

## 5. Conclusion

The present work has demonstrated the potential for the fabrication of thermal barriers by electrodeposition on a metal conversion coating substrate. The electrochemical method offers a relatively easy way to control the thickness and composition gradients which characterize such coatings. These composition gradients must induce a gradual variation of thermal and physical properties from the metallic substrate up to the surface and explain the good coat adhesion noted at high temperature. Conversion coatings modified in this way with metal oxide ceramic are also promising for catalytic applications, as an alternative solution to the traditional alumina washcoat layer on a metal substrate and as support of thin films with particular properties (e.g. superconductivity) obtained by advanced techniques (e.g. CVD).

## References


[1] T. E. Shmid and R. Y. Hecht, *Ceram. Eng. Sci. Proc.* **9** (1988) 1089.
[2] C. R. Aita, *Mater. Sci. Technol.* **8** (1992) 666.
[3] M. Shane and M. L. Mecartney, *J. Mater. Sci.* **25** (1990) 1537.
[4] D. E. Clark, W. J. Dalzell and D. C. Folz, *Ceram. Eng. Sci. Pro.* **9** (1988) 1111.
[5] E. N. Balko and P. H. Nguyen, *J. Appl. Electrochem.* **21** (1991) 678.
[6] G. E. F. Brewer, *Am. Ceram. Sci. Bull.* **51** (1972) 216.
[7] D. Tench and L. Warren, *J. Electrochem. Soc.* **130** (1983) 869.
[8] M. Sakai, T. Sekine and Y. Yamazaki, *J. Electrochem. Soc.* **130** (1983) 1631.
[9] J. A. Switzer, *J. Electrochem. Soc.* **133** (1986) 722.
[10] *Idem, Am. Ceram. Soc. Bull.* **66** (1987) 1521.
[11] L. Gal-Or, I. Silberman and R. Chaim, *J. Electrochem. Soc.* **138**(7) (1991) 1939.
[12] R. Chaim, I. Silberman and L. Gal-Or, *ibid.* **138**(7) (1991) 1942.
[13] G. Aguilar, J. C. Colson and J. P. Larpin, *Mem. Sci. Rev. Met.* **7–8** (1992) 447.
[14] M. M. Hefny, *J. Appl. Electrochem.* **21** (1991) 485.
[15] L. Aries and H. Triche, *C. R. Acad. Sci.* **264** (1967) 1236.
[16] *Idem, Mem. Sci. Rev. Met.* **7–8** (1967) 669.
[17] *Idem, ibid.* **10** (1968) 761.
[18] L. Aries, J. P. Bonino, R. Benavente and J. P. Traverse, *Mat. Res. Bull.* **18** (1983) 791.
[19] L. Aries, Y. Baziard, D. Fraysse and J. P. Traverse, *Solar Energy* **36** (1986) 521.
[20] L. Aries, J. Roy, T. Bouissou and R. Sempere, *Mat. Sci. Tec.* **7** (1991) 24.
[21] L. Aries, J. Roy, B. Naboulsi, T. Bouissou and R. Sempere, *ibid.* **7** (1991) 757.
[22] L. Aries, M. El Bakkouri, J. Roy, J. P. Traverse, R. Calsou and R. Sempere, *Thin Solid Films* **197** (1991) 143.
[23] L. Aries, J. A. Flores, J. Roy and R. Calsou, *Br. Corros. J.* **25** (1990) 299.
[24] J. K. Walker, J. Kinkoph and C. K. Saha, *J. Appl. Electrochem.* **19** (1989) 225.
[25] S. C. Tjong, *Werkst. Korros.* **37** (1986) 591.